Nonscattered states in a random-dimer model

P. K. Datta, D. Giri, and K. Kundu*
Institute of Physics, Bhubaneswar 751005, India
(Received 17 August 1992)

We study a random-dimer model within the context of a tight-binding Hamiltonian in one dimension. This model may be useful in understanding the transport properties of the polyaniline system. As a prelude to our understanding we consider a few simple but relevant models. For these cases we investigate the behavior of the phase of the transmission coefficient. From the study of these models we conclude that many resonances merge around the dimer energy in the random-dimer model. Our subsequent analysis of the random-dimer model proves this conjecture. This analysis, however, does not yield the number of nonscattered states in the system. According to Dunlap, Wu, and Phillips [Phys. Rev. Lett. **65**, 88 (1990)] there will be $\sqrt{N}$ nonscattered states around the dimer energy. To obtain the number of nonscattered states we study the transmission coefficient. We find that the averaged transmission coefficient yields approximately a Lorentzian curve. Furthermore, there is an energy width where the transmission coefficient is approximately unity. For a high concentration of dimers and dimer energy well inside the host band we find $\sqrt{N}$ nonscattered states. A similar number of nonscattered states is obtained for a low concentration of dimers and dimer energy near the band edge. In general we find a discernable discrepancy between the observed half-width and the calculated half-width. The discrepancy is quite significant when the dimer energy is close to one of the band edges. On the basis of these results we speculate that the averaged half-width scales as $N^{-\lambda}$ when λ is a function of both the concentration and the energy of the dimer.

I. INTRODUCTION

In recent years the field of conducting polymers has been of immense interest. Generally, polymers are nonconductors. The doped form of polymers, however, can show high conductivity due to the degeneracy of the ground state.[1,2] An example in this regard is polyacetylene. Although polymers such as polyaniline, polypyrolle, etc., lack degenerate ground states, they show high conductivity on doping.[3–6] Two parent forms of polyaniline containing benzenoid rings and a mixture of benzenoid and quinoid rings are leucoemeraldine and emeraldine, respectively. The electrochemical oxidation of the leucoemeraldine or acidification of the emeraldine shows an insulator-metal transition. Electron spin resonance and NMR studies[6] suggest that polyaniline is a one-dimensional conductor. The first theoretical calculation of the electronic structure of polyaniline containing nearly 200 benzenoid rings and randomly placed quinoid rings were performed by Galvao *et al.*[7] In as much as the calculation of Galvao *et al.* indicates that upon protonation of emeraldine, the Fermi level moves to a region where the conducting states are located, Wu and Phillips[8,9] believe that the transport properties of polyaniline can be understood from the analysis of the random dimer model (RDM).[10,11] They, in fact, mapped the polyaniline system to a RDM. It therefore appears that the essential features of polyaniline can be understood in terms of a RDM. This then necessitates a thorough analysis of the RDM. Our present work is an attempt in that direction.

To understand the interesting features of the model, some knowledge of Anderson's localization in disordered systems is necessary. The well-known result in the Anderson model[12] for the site-energy disorder is the absence of long-range transport in one-dimensional systems. It has been conjectured that all solutions of the Schrödinger equation are exponentially localized.[13] This result is supported by other works.[14–18] The effect of exponentially localized eigenstates can be observed in the exponential decay of the transmission coefficient with the length of the system.[19,20] Also, for a one-dimensional binary distribution of site energies, many resonance peaks appeared in the transmission coefficient[20] with large localization length.[21] The basic idea of these discussions is that almost all the states are exponentially localized in a one-dimensional system of randomly distributed site energies. There are, however, examples of one-dimensional disordered systems where the existence of extended states has been observed. The one-dimensional-liquid model shows the existence of nonlocalized states.[22] The off-diagonal disorder also produces extended states around the middle of the band.[23] The study of a one-dimensional site-energy disorder problem with a particular distribution shows a new band of states having localization length $\sim\sqrt{N}$, where N is the length of the system.[24] One can also include in this category one-dimensional quasiperiodic systems containing Cantor-type spectra and critical states.[25–27] Other examples will be systems having correlated diagonal and off-diagonal disorders. For these systems, Flores[28] showed the existence of critical energy (E_c) for transport. The energy width (ΔE) goes as $1/\sqrt{N}$, and the Lyapunov exponent is $\sim(E-E_c)^2$ for E inside the band. Also, the mean-square displacement calculation shows the superdiffusive behavior in transport [29] for a particle having energy inside the band. RDM can be shown to be an example of the correlated diagonal and

off-diagonal disordered systems.[10,11]

RDM is a one-dimensional correlated random binary alloy with the site energies ϵ_a and ϵ_b. The energy ϵ_a is assigned to a pair, called a dimer, distributed randomly in the system. The constant nearest-neighbor interaction is V which mediates transport from one site to its nearest site. Of course, the system is assumed to be described by Anderson's tight-binding Hamiltonian.[12] Dunlap, Wu, and Phillips [henceforth referred to as DWP (Ref. 10)] showed that the reflection coefficient of a system containing a single dimer vanishes provided $|\epsilon_a-\epsilon_b|\leq 2V$. On the basis of this interest they claimed that RDM has $\sqrt{N}$ states which extend over the whole sample. Here, N is the number of sites in the system. They also numerically calculated the mean-square displacement for excitations localized initially on a site. They found that the mean-square displacement grows as $t^{3/2}$ if $|\epsilon_a-\epsilon_b|<2V$. On the other hand, if $|\epsilon_a-\epsilon_b|=2V$, the motion is diffusive. The behavior of the mean-square displacement has been cited as supporting evidence for their claim. Also, Wu and Phillips described some other one-dimensional systems,[30,31] for example; (1) a random-n-mer model, (2) a repulsive binary alloy, (3) a random bipolaron lattice, and (4) a random soliton lattice. These models are closely related to the RDM. The perturbative calculation of the density of states and the Lyapunov exponent in the vicinity of the dimer energy shows the existence of nonscattered states.[32] Again, the claim is that there are $\sqrt{N}$ such states. Gangopadhyay and Sen[33(a)] have studied numerically a system containing randomly placed double dimers. For this system, they found that there are $N^{1/3}$ ballistic states. Furthermore, according to Gangopadhyay and Sen, the number of states having a localization length equal to or larger than the sample size is roughly proportional to $\sqrt{N}$. They further claim that the superdiffusive and diffusive behavior of the mean-square displacement is a short-time phenomenon.[33(b)]

In all these discussions[8-11,31] it has been tacitly assumed that the number of nonscattered states in RDM does not depend either on the dimer energy or the concentration of dimers in the chain. The rationale behind it is that the fraction of such states is infinitesimal. Furthermore, all the calculations yield an order-of-magnitude estimation of the number of conducting states. Therefore, it can be argued that any weak variation in this number can be accommodated in the margin of estimation. Note, however, that the Lyapunov exponent of such states does show a strong dependence on the dimer energy. We therefore expect this number to show a perceptible dependence on the above two parameters. This can be observed by careful numerical analysis of say, the transmission coefficient. Keeping this in mind we study here the dependence of the number of nonscattered states on the dimer energy and its concentration in the chain numerically. We also check our numerical results by studying a few simple but relevant models analytically.

This paper is organized as follows. In Sec. II, we introduce our simple models to understand the origin of the nonscattered states. We also derive here the general formula for the transmission amplitude. In Sec. III, we calculate the transmission coefficient for these models. Here, we also study the dependence of the phase of the transmission coefficient on the particle energy. This quantity evaluated at the resonance energy may yield the width of the resonance state. This study is useful for understanding the behavior of RDM. In Sec. IV, we examine the transmission coefficient of RDM containing a very large number of sites. From this we calculate the width of nonscattered states for different dimer energies and concentrations. For different dimer energies and concentrations, the number of nonscattered states around the dimer energy is described in Sec. V. In Sec. VI, we summarize our essential results.

II. MODEL

The Hamiltonian (H) for the models described later is the well-known tight-binding type with nearest-neighbor interactions,

$$H=\sum_i \epsilon_i a_i^\dagger a_i+\sum_{\langle i,j\rangle} V_{ij} a_i^\dagger a_j \ , \tag{1}$$

where $a_i^\dagger$ is the electron creation operator in the ith localized orbital, ϵ_i is the energy of the ith orbital, and V_{ij} is the nearest-neighbor tunneling matrix element. In our model all nearest-neighbor interactions are of equal strength, say V. Since all the relevant energies can be scaled by V, without loss of generality we can set V to unity. For the dimer site, the site energy is ϵ_a with sites coming in pairs. The energy of the perfect site is ϵ_b. In as much as the dynamics of the system is governed by the difference in energy of the two types of sites, we set the dimer site energies as $\epsilon_0=\epsilon_a-\epsilon_b$ and zero to the perfect sites.

We examine the dynamics of the system by studying the behavior of the transmission coefficient. We use analytical as well as numerical methods. We have a system containing N sites connected from both sides to semi-infinite chains consisting of perfect sites. Our system may consist of (a) a continuous dimer, (b) two segments of equal length of continuous dimers separated by a string of perfect sites, (c) a regular arrangement of dimer-perfect sites, and (d) a random arrangement of dimer and perfect sites. All these models have been described in appropriate places. The general site amplitude equation for the system is given by

$$i\frac{dc_n}{d\tau}=\epsilon_n c_n+c_{n+1}+c_{n-1} \ , \tag{2}$$

where $c_n(\tau)$ is the amplitude at the nth site at time τ, and $\epsilon_n=\epsilon_0$ or 0 as mentioned before. The Fourier transform of Eq. (2) can be written as

$$X_{n+1}=P_n X_n \ , \tag{3}$$

where P_n is a $SL(2,R)$ (Ref. 26) matrix with the representation

$$P_n=\begin{bmatrix} E-\epsilon_n & -1 \\ 1 & 0 \end{bmatrix} ,$$

which is usually called the transfer matrix. Here, X_n is a column vector comprised of $c_n(E)$ and $c_{n-1}(E)$. $c_n(E)$ is the Fourier transform of $c_n(\tau)$.

To calculate the transmission amplitude t of a segment containing N sites, we number the sites in the system from the left end starting with 1. We shoot a particle form $-\infty$ with $E=2\cos k$ towards the sample. While the particle passes through the sample it undergoes multiple elastic scattering. Eventually, it comes out of the sample from the right end with amplitude t. The general process is shown in Fig. 1.

Following Liu and Chao[34] we write the site amplitude as

$$c_n=\begin{cases} f_{k+>}e^{ikn}+f_{k->}e^{-ikn} & \text{for } n\geq N \\ f_{k+<}e^{ikn}+f_{k-<}e^{-ikn} & \text{for } n\leq 0 \end{cases}.$$

Then Eq. (3) reduces to

$$\begin{bmatrix} f_{k+>} \\ f_{k->} \end{bmatrix}=Q(k,N)\begin{bmatrix} f_{k+<} \\ f_{k-<} \end{bmatrix}, \tag{4}$$

where

$$Q(k,N)=\begin{bmatrix} e^{-ikN} & 0 \\ 0 & e^{ikN} \end{bmatrix}S^{-1}\prod_{i=1}^{N}P_nS$$

and

$$S=\begin{bmatrix} e^{ik} & e^{-ik} \\ 1 & 1 \end{bmatrix}.$$

We are considering the wave coming from the left side. There is no backward wave on the right side. So, we set $f_{k->}=0$. Then, from Eq. (4), we readily obtain

$$t=\frac{f_{k+>}}{f_{k+<}}=\frac{\Delta}{[Q(k,N)]_{22}}, \tag{5}$$

where

$$\Delta=\det[Q(k,N)].$$

III. PHASE ANALYSIS

Since in a RDM $|t|^2$ is always unity at $E=\epsilon_0$, the system has a resonance state at this energy. Therefore we expect this state to have a well-defined width. This width can be obtained by the phase analysis.[35] To understand the basic concept of phase analysis, we consider a one-dimensional square well of a uniform depth V_0 and of width a which extends to the positive direction of the origin. The transmission amplitude of a free particle with energy $E>0$ for this particular problem is

$$t=\left[\cos\bar{p}a-\frac{i}{2}\left[\frac{p}{\bar{p}}+\frac{\bar{p}}{p}\right]\sin\bar{p}a\right]^{-1}e^{-ipa}=S(E)e^{i\theta}, \tag{6}$$

where $\theta=-pa$, $p=\sqrt{E}$, and $\bar{p}=\sqrt{E+|V_0|}$, taking $2m=\hbar=1$.

It can be readily seen that this system has resonance at $E_r=n^2\pi^2/a^2-|V_0|>0$ where n is an integer greater than zero. Since resonance appears as a complex pole of $S(E)$ in the second Rieman sheet of the complex E plane, the width of the resonance can be obtained by examining the behavior of the phase of $S(E)$, that is $\phi(E)$, at the resonance energy. It can be shown from standard analysis that

$$\left.\frac{d\phi}{dE}\right|_{E=E_r}=\frac{2}{\Gamma}. \tag{7}$$

Furthermore, both $|t|^2$ and $d\phi/dE$ as functions of E will yield Lorentzian curves. The half width of the transmission coefficient curve is Γ. These two quantities have maximum values at the resonance energy.

We now analyze the transmission amplitude t for a system containing a single dimer,

$$t(E)=S(E)e^{i(-2k\pm\pi)} \tag{8}$$

with

$$S(E)=\frac{2i\sin k}{2i\sin k+(E-\epsilon_0)^2e^{-ik}-2(E-\epsilon_0)}. \tag{9}$$

Since $E=2\cos k$, we have a perfect resonance, i.e., $|t|^2=1$ at the dimer energy ϵ_0 provided $|\epsilon_0|\leq 2$. So, in all calculations, we define $\epsilon_0=2\cos k_0$. We calculate the width of the resonance (Γ) at ϵ_0 by a Taylor series expansion of $S(E)$ in terms of $(E-\epsilon_0)$. In the leading-order approximation,

$$t\sim\frac{e^{i(-2k\pm\pi)}i\Gamma/2}{(E-\epsilon_0)+i\Gamma/2}, \tag{10}$$

where the resonance width $\Gamma=|2\sin k_0|=\sqrt{4-\epsilon_0^2}$. In this context we would like to mention one important point about the direction of wave propagation. Since the energy associated with the wave is $E=2\cos k$, it has no phase velocity. So, the direction of propagation is defined by a group velocity which is $-2\sin k$. Hence, one needs to choose an appropriate sign of k to determine the phase of the transmission amplitude (t).

The resonance width indicates that there will be a peak in $d\phi/dE$ at the dimer energy with a peak value of $2/\Gamma$. But in the system with a single dimer $d\phi/dE$ does not show any peak at this energy. This behavior is exactly what is observed in the one-dimensional square-well problem with small width and depth. Differences arise due to the finite bandwidth effect. For example, the band edges of the host crystal in this case correspond to the

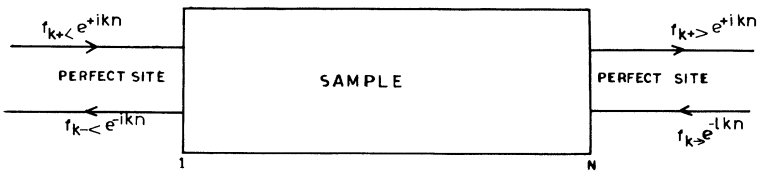

FIG. 1. Schematic diagram of our model. In all cases the sample starts and ends with the dimer.

low-energy part of the square-well problem. Therefore, resonance peaks appear first near the band edges. In other words, $d\phi/dE$ should have maxima at the band edges. Furthermore, here the continuous spectra are symmetrically disposed from -2 to 2. Hence, $d\phi/dE$ decreases from both sides and eventually the two curves meet at some interior point. This point is, of course, determined by the dimer energy. In the case of a one-dimensional (1D) square well with small depth and width, $d\phi/dE$ continuously decreases from zero energy. It is also known that in the 1D square-well problem, peaks in the transmission coefficient are obtained either by increasing the width or the depth of the well. Therefore if we increase the length of the dimer segment, the similarity between these two problems can be understood. We next study the case of a segment containing more than one dimer.

A. Continuous-dimer model

Here we are considering a regular arrangement of p $(=N/2)$ number of dimers in the sample containing N sites. We have seen for single dimer scattering that the phase is $\theta=-2k\pm\pi$ at the dimer energy. It is interesting that the phase is coherently built up and can be seen in the analytical calculation presented below. For this segment of continuous dimer, the phase is $\theta=p(-2k\pm\pi)$. We obtain the transmission amplitude,

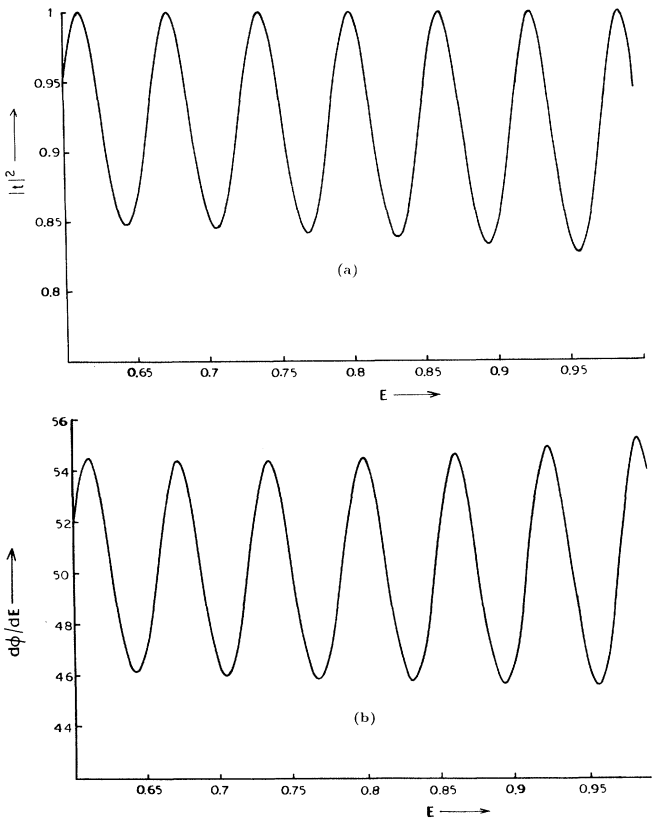

FIG. 2. (a) Transmission coefficient ($|t|^2$) as a function of particle energy (E) for model (a) with a segment containing 50 dimers and $\epsilon_0=0.8$. (b) Plot of $d\phi/dE$ vs E for the system described in (a).

$$t=S(E)e^{ip(-2k\pm\pi)}=\frac{-(2i\sin k)e^{-(ikN)}}{[(B-C)+Ae^{-ik}-De^{ik}]} \tag{11}$$

and

$$S(E)=|S(E)|e^{i\phi} ,$$

where

$$A=\frac{\sinh(N+1)\xi}{\sinh\xi} ,$$

$$B=-C=-\frac{\sinh N\xi}{\sinh\xi} ,$$

$$D=-\frac{\sinh(N-1)\xi}{\sinh\xi} ,$$

and

$$2\cosh\xi=(E-\epsilon_0) .$$

It can be easily shown that at the dimer energy, $|t|^2=1$ and the phase is given by

$$\phi=\tan^{-1}\left[\frac{\mathrm{Im}S(E)}{\mathrm{Re}S(E)}\right] .$$

The behavior of $|t|^2$ and $d\phi/dE$ around the dimer energy for $N=100$ and $\epsilon_0=0.8$ obtained from this analytical calculation is shown in Figs. 2(a) and 2(b). Also, there are many sharp resonance peaks in $|t|^2$ and $d\phi/dE$ around the dimer energy. It can be shown that the resonance width (Γ) at ϵ_0 goes as $1/N$, where N is the number of sites. If we assume that the Bloch k is a good quantum number of the system, the number of states encompassed at ϵ_0 is unity. This statement holds for all other resonances in the system. Let us denote the component of the dimer by A. Instead of taking an even number of A sites, if we take an odd number of such sites, we see the same structure of $|t|^2$ but there is no peak at the energy of the site of the A type. If we subtract the proper phase at the resonance energies, we expect maxima of $d\phi/dE$ at those resonance energies. We also find, although it is not shown, that the peaks in $|t|^2$ become closer and sharper with the increase in the number of dimers with a tendency to form a band around the dimer energy.

B. Dimer-perfect-dimer model

In this model, m number of perfect sites are flanked from both sides by segments containing p number of dimers in each one of them. This model is equivalent to the resonance tunneling through a double barrier in one dimension. This can be used to understand the conduction in semiconductors consisting of $Al_xGa_{1-x}As$ as barrier layers with GaAs in the well and contacts.[36] The transmission coefficient for the system is the same as in Eq. (11) with

$$A=\frac{1}{\sinh^2\xi\sinh\xi'}[\sinh^2(2p+1)\xi\sinh(m+1)\xi'-2\sinh 2p\xi\sinh(2p+1)\xi\sinh m\xi'+\sinh^2 2p\xi\sinh(m-1)\xi'],$$

$$B=-C=\frac{1}{\sinh^2\xi\sinh\xi'}[-\sinh 2p\xi\sinh(2p+1)\xi\sinh(m+1)\xi'+\sinh^2 2p\xi\sinh m\xi'$$
$$+\sinh(2p-1)\xi\sinh(2p+1)\xi\sinh m\xi'-\sinh 2p\xi\sinh(2p-1)\xi\sinh(m-1)\xi'],$$

and

$$D=\frac{1}{\sinh^2\xi\sinh\xi'}[-\sinh^2 2p\xi\sinh(m+1)\xi'+2\sinh 2p\xi\sinh(2p-1)\xi\sinh m\xi'-\sinh^2(2p-1)\xi\sinh(m-1)\xi'],$$

where $2\cosh\xi=(E-\epsilon_0)$ and $2\cosh\xi'=E$.

This system is analogous to the system of the continuous dimer if we remove the perfect-site chain. If we put just one perfect site in between two continuous-dimer segments, we observe broadness in the transmission peak around the dimer energy as well as in other resonance peaks [see Fig. 3(a)]. This is due to the merging of resonance peaks. Again, with the increase in the number of perfect sites, the other resonance peaks sharpen faster and this number also increases. Of course, the distance between resonance peaks also decreases. At the same time the width of $|t|^2$ around ϵ_0 decreases. The same behavior is observed if we increase the length of the continuous dimer by keeping the number of perfect sites fixed.

Since resonance states in this system can cluster around the dimer energy, the derivative of the phase with respect to the energy ($d\phi/dE$) may not always yield a maximum at the resonance energy. This is exactly what we observe in Fig. 3(b). Also note that as we increase the number of dimer sites as well as perfect sites, $d\phi/dE$ also starts yielding a Lorentzian shape with a maximum at the resonance energy [see Fig. 3(c)]. We should also mention that $d\phi/dE$ around ϵ_0 goes as N. The observed behavior of the system can be nicely explained by invoking an interaction between the energy interfaces, which decreases strongly with increasing the distance between the interfaces. For example, if we increase the length of the intervening perfect sites by keeping the length of the dimer segments fixed, the distance between two interfaces connecting the dimer chains to the perfect chain will increase. This will, in turn, reduce the interaction between these two interfaces. Consequently, we should expect sharp resonance peaks around the dimer energy. This is actually observed. Similarly, if we increase the length of the dimer chain the distance between interfaces separating the dimer chains from the perfect sites will increase. So the peaks should sharpen according to our theory. This is also observed.

C. Regular arrangement of the dimer-perfect-site model

Here we consider a regular arrangement of the dimer-perfect site in the sample of length N. So, the number of units of the dimer-perfect site is p ($=N/3$). For each unit the phase in the transmission coefficient is $-2k\pm\pi$ at the dimer energy and consequently for p units, it will be $(-2k\pm\pi)p$. The transmission coefficient for this system is the same as Eq. (11) with redefined coefficients A,

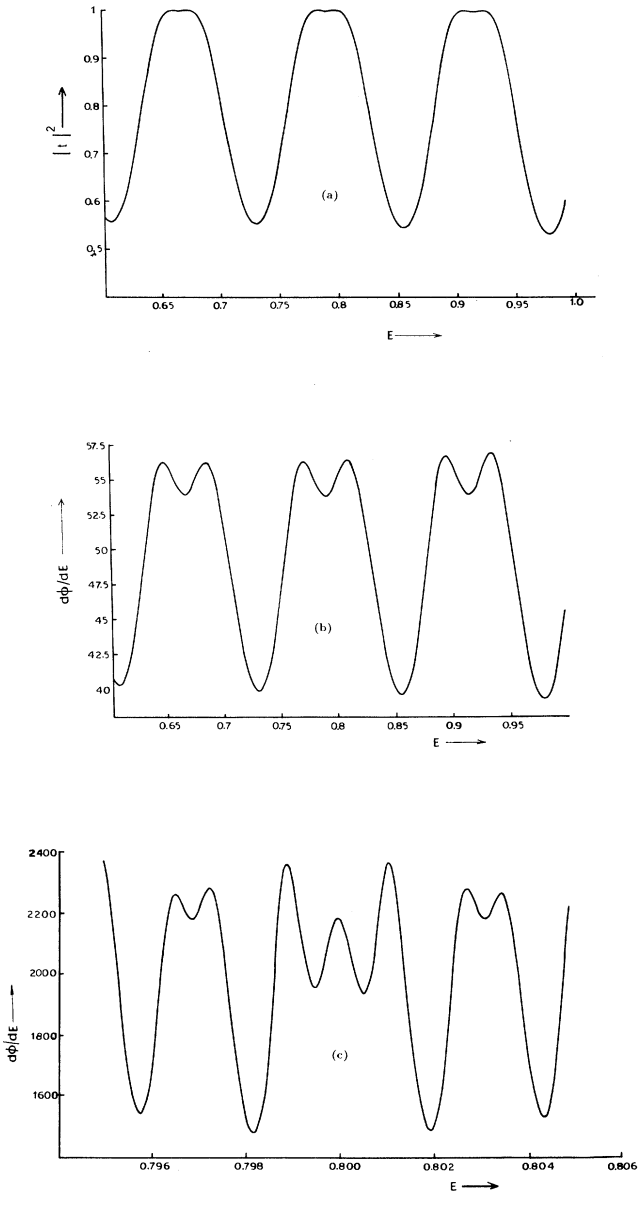

FIG. 3. (a) Variation of $|t|^2$ with E for model (b) with two dimer segments containing 25 dimers each and 1 perfect site in between. The dimer energy is $\epsilon_0=0.8$. (b) Variation of $d\phi/dE$ with E for the system described in (a). (c) Plot of $d\phi/dE$ vs E for model (b) with two dimer segments containing 1000 dimers each and 1000 perfect sites in between with $\epsilon_0=0.8$.

B, C, and D where

$$A=\frac{\sinh(p+1)\xi-(E-\epsilon_0)\sinh p\xi}{\sinh\xi},$$

$$B=\frac{[E(E-\epsilon_0)-1]\sinh p\xi}{\sinh\xi},$$

$$C=\frac{[1-(E-\epsilon_0)^2]\sinh p\xi}{\sinh\xi},$$

$$D=\frac{-\sinh(p-1)\xi+(E-\epsilon_0)\sinh p\xi}{\sinh\xi},$$

and $2\cosh\xi=E+2(E-\epsilon_0)-E(E-\epsilon_0)^2$.

Also for this case, $|t|^2=1$ at the dimer energy. Since two dimers here are separated by a perfect site, the interaction between the interfaces should be large. This will, in turn, cause the resonance peaks to merge around the dimer energy. This is observed both in the transmission coefficient and in $d\phi/dE$ as shown in Figs. 4(a) and 4(b). The important difference here is that we always obtain an energy width (ΔE) where the transmission coefficient is approximately unity. Furthermore, this is a periodic system with a periodicity of three. So, when the length of the segment goes to infinity we must obtain three bands.[25] This is also obtained in our calculations.

D. Random-dimer model

This system contains randomly placed dimer and perfect sites. Since the RDM is an intermediate case of the second and third model, we also expect the merging of resonances here. In our numerical results we see the transmission resonance peaks merging around the dimer energy. To subtract the proper phase at the energy we use the following numerical method. We know that for a single dimer case, the phase is $\theta=-2k\pm\pi$. If there are p number of dimers, the phase is $\theta=(-2k\pm\pi)p$ at the dimer energy. Second, we can change the position of the resonance energy by changing the dimer energy. If we define the transmission amplitude for a particle with energy E in the RDM with dimer energy ϵ_0 and E as $t(E,\epsilon_0)$ and $t(E,E)$, respectively, then the ratio of $t(E,\epsilon_0)$ and $t(E,E)$ cancels the extra phase of the transmission amplitude at that energy. $d\phi/dE$ around ϵ_0 has been calculated for different realizations of a sample as well as for different chain lengths. In all cases our numerical analysis shows the absence of a maximum in $d\phi/dE$ at ϵ_0. A typical result is shown in Fig. 5. Note also that $d\phi/dE$ at ϵ_0 goes as N, where N is the number of sites. This is the maximum possible value of this quantity. Note also for the continuous-dimer case that the value of $d\phi/dE$ at ϵ_0 goes as N. This has been mentioned before. Therefore, if the system shows a sharp resonance at ϵ_0 after some value of N, the width of the resonance cannot be less than $1/N$. Hence, this system must contain at least one extended state. Furthermore, the absence of a maximum in $d\phi/dE$ at ϵ_0 is a strong indication of the merging of resonance states around the dimer energy. The merging of resonance states around ϵ_0 can be understood by noting that the transfer matrix of a dimer around the dimer energy is almost a unit matrix. Hence, in the small neighborhood of energy, the full system will behave as like an infinite system of perfect sites. Consequently, there should be more than one extended state in the vicinity of the dimer energy. Of course, from this analysis, we do not obtain the width of such states. In the next section we therefore focus our attention on the numerical calculation of the transmission coefficient of RDM.

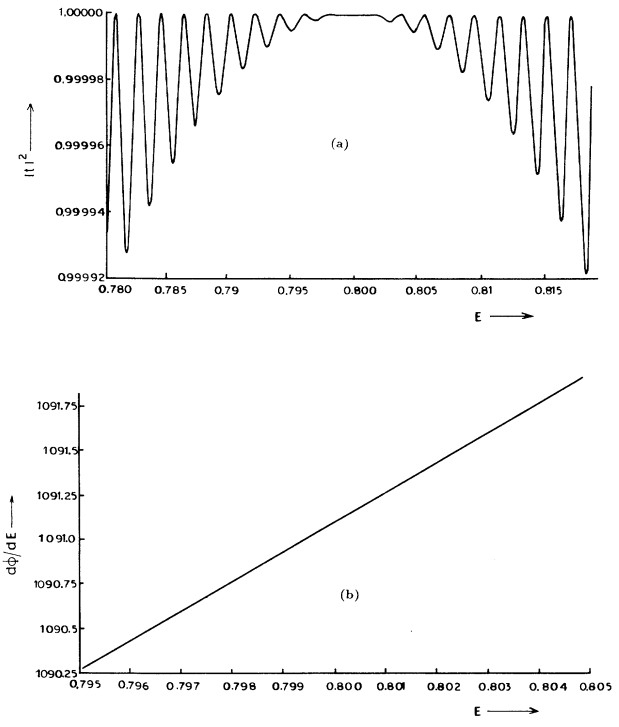

FIG. 4. (a) $|t|^2$ as a function of E for model (c) containing 1000 units of dimer-perfect sites with dimer energy 0.8. (b) Plot of $d\phi/dE$ vs E for the system described in (a).

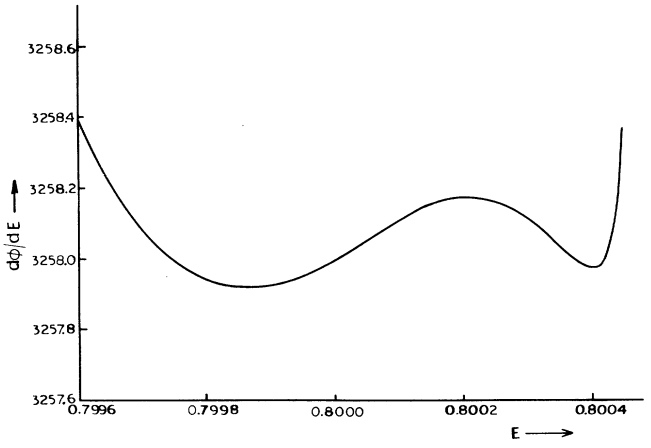

FIG. 5. Plot of $d\phi/dE$ vs E for RDM with sites 9000. The dimer energy is 0.8 and the dimer concentration is $\rho=0.33$.

IV. TRANSMISSION COEFFICIENT ANALYSIS

The behavior of $d\phi/dE$ around ϵ_0 in RDM clearly indicates the presence of more than one nonscattered state in the vicinity of interest. We cannot, however, say from phase analysis whether or not there are $\sqrt{N}$ nonscattered states in the sample. Here, N is the number of sites in the sample. Of course, the above number is obtained by an analytical method.[8-11,30,31] We should mention that certain assumptions are made to obtain the result. These assumptions may not hold true for this type of system. Furthermore, the system may have other important features which may not be obtained by analytical methods. For example, the system may contain many other resonance states. The number of nonscattered states may depend on the dimer energy and the concentration of the dimers in the sample. Hence, this problem should be thoroughly investigated by numerical techniques.

To have a better understanding of the problem, we first analyze the transmission coefficient of a system of random dimers containing N sites along the line of Dunlap, Wu, and Phillips.[10] The reflection coefficient $|r|^2$ for a single dimer is

$$|r|^2=\frac{\epsilon_0^2(\epsilon_0-2\cos k)^2}{4\sin^2 k+\epsilon_0^2(\epsilon_0-2\cos k)^2} . \tag{12}$$

The reflection coefficient vanishes at $\epsilon_0=2\cos k$, i.e., when the dimer energy is equal to the particle energy. Expanding $|r|^2$ around $k_0=\cos^{-1}(\epsilon_0/2)$, which is well inside the host of the perfect-site band, and keeping the lowest-order term we can write

$$|r|^2\approx\beta(k_0)(\Delta k)^2 , \tag{13}$$

where $\beta(k_0)$ is a coefficient of $(\Delta k)^2$ in the expansion of $|r|^2$. We consider now a sample of length N containing a randomly placed p number of dimers and a $N-2p$ number of perfect sites. Around the dimer energy, as the reflection coefficient is small, we neglect the backscattering effect due to each dimer. Then, within this approximation, we can write

$$|T|^2\approx|t|^{2p} . \tag{14}$$

Here, $|T|^2$ is the total transmission coefficient of the segment under consideration and $|t|^2$ is the transmission coefficient for the single dimer problem. Since $|t|^2=1-|r|^2$, it can be shown that

$$|t|^{2p}=\exp\left[-p\sum_{q=1}^{\infty}|r|^{2q}/q\right] . \tag{15}$$

As $|r|^2\ll 1$, keeping only the first term in the summation, we obtain

$$|T|^2\approx e^{-p|r|^2}\approx e^{-\rho\beta(k_0)N(\Delta k)^2} , \tag{16}$$

where ρ is the concentration of the dimers $=p/N$. We now consider a region of $\Delta k=c/N^{\alpha}$, with $0<\alpha<1$ around ϵ_0. Thus,

$$|T|^2\approx e^{-\rho\beta(k_0)c^2/N^{2\alpha-1}} . \tag{17}$$

We consider now different cases for the large N limit,

(1) for $\alpha<\frac{1}{2}$, $|T|^2\to 0$ as $N\to\infty$

(2) for $\alpha=\frac{1}{2}$, $|T|^2\sim e^{-\rho\beta(k_0)c^2}$

which is independent of N

(3) for $\alpha>\frac{1}{2}$, $|T|^2\to 1$ as $N\to\infty$.

Since the unperturbed state is $k=2\pi l/N$, $l=0,\pm1,\pm2,\ldots$, the integer values of $\alpha>1$ need not be considered and the physically relevant range of α is $(\frac{1}{2}\le\alpha<1)$. So, from this simple proof, we see that if there are states at $k=k_0+c/N^{\alpha}$ $(\frac{1}{2}\le\alpha<1)$ where c is $O(1)$, these states are totally transmitting. Let us assume now that $\Delta k=2\pi\Delta N/N^{\delta}$, where the parameter δ can take a value between $\frac{1}{2}$ and 1. When $\delta=1$, we get a Bloch wave vector. Furthermore, in this situation, $\frac{1}{2}\le\alpha<\delta$. After equating two expressions for Δk, we obtain $|\Delta N|\sim N^{(\delta-\alpha)}$. The maximum number of nonscattered states is obtained if $\alpha=\frac{1}{2}$. So, within our approximation, we obtain the maximum number of nonscattered states if all states in the width are Bloch-type extended states. The result of Ref. 10 is a special case of our analysis. We next analyze the Lyapunov exponent of these nonscattered states.

The transmission coefficient for a single dimer around ϵ_0 in ΔE $(=|E-\epsilon_0|)$ can be obtained from Eq. (10) and it is

$$|t|^2\sim\frac{1}{1+\dfrac{(E-\epsilon_0)^2}{\Gamma^2/4}} . \tag{18}$$

If we employ the same analysis here as we did before to obtain the number of nonscattered states we get

$$|T|^2\approx e^{-(4/\Gamma^2)\rho N(E-\epsilon_0)^2} . \tag{19}$$

Equation (19) can be equivalently written as

$$|T|^2\sim e^{-(N/N_0)} , \tag{20}$$

where the Lyapunov exponent, which is the inverse of the localization length (N_0), is obtained as $\gamma\approx\rho(4/\Gamma^2)(E-\epsilon_0)^2$.[32] We also obtain the effective resonance width (Γ_{eff}) at ϵ_0 for RDM given by $\Gamma/\sqrt{\rho N}$. This is true if ϵ_0 is well inside the parent band, where Γ for the single dimer case is finite. Note that the Lyapunov exponent vanishes at the dimer energy. However, the vanishing Lyapunov exponent does not necessarily imply that it is a Bloch-type extended state. It can very well be a critical state.[26] If it is a Bloch-type state it cannot appear as a single state. Otherwise, it will be a point spectrum and the state will be localized. The behavior of $d\phi/dE$ around ϵ_0 also supports this argument. Furthermore, if ϵ_0 is close to one of the band edges, a careful analysis of our expression for the Lyapunov exponent yields $\gamma\approx\rho|E-\epsilon_0|$. This result is also consistent with the result of Ref. 32. It should also be noted that if ϵ_0 is at the band edge, γ will be zero there and infinity in the vicinity. Also, in this case, Γ_{eff} is zero.

This implies that when ϵ_0 is at one of the band edges there will be only one state with a localization length larger than the sample size. Since $\gamma=0$ for this state, it is a critical state.[26] In the subsequent section we check the validity of our analysis by numerical calculation of the transmission coefficient for very large segments.

In Figs. 6(a)–6(d) we have plotted the transmission coefficient as a function of the incident particle energy for different concentrations and dimer energies for a large, but finite, size of the sample ($\sim 10^5$). The smooth curve corresponds to $|t|^{2p}$. We also show the sample-averaged behavior of the transmission coefficient [Figs. 7(a)–7(d)] as a function of particle energy for different concentrations and dimer energies for samples of length $\sim 10^4$. The dotted curve represents $\langle |t|^{2p} \rangle$ and the smooth solid curve represents

$$\left\langle \frac{1}{1+4(E-\epsilon_0)^2/\Gamma_{\text{eff}}^2} \right\rangle .$$

Here, the average has been taken because of the fluctuation, albeit small, in the number of dimers in the sample. We performed arithmetic averaging with ten samples. We consider first the case of low concentration and dimer energy well within the parent band, for example, $\rho=0.33$ and $\epsilon_0=0.8$. Note that the sample contains an energy width (ΔE) where the transmission coefficient is of the order of unity. Furthermore, this width is of the order of $1/\sqrt{N}$. It is independent of the configuration of the sample. The presence of this width can be understood by noting that at $E=\epsilon_0$, the dimer transfer matrix is unity. Since both the connecting blocks and the disordered segments contain the same elements, at $E=\epsilon_0$, the sample will be a perfect crystal of infinite length. As long as E is not very different from ϵ_0, the perfectness of the system is approximately preserved. This is precisely the origin of the configuration-independent width ΔE. It is also equally noteworthy that there is a lot of sharp resonances beyond this region in every sample. But the averaged transmission coefficient shows almost a Lorentzian shape with a half-width of Γ_{fig}. This width, however, is larger than Γ_{eff}. Furthermore, the actual half-width (Γ_{fig}) is roughly an order of magnitude larger than the width of the regime (ΔE).

Although the extra resonances averaged out, these states may contribute significantly to the mean-square displacement. Furthermore, we should also mention that transmission peaks become sharper and closer to each other around the dimer energy, if we increase the size of the sample. The number of such peaks also increases. This interesting feature is exactly same as whatever we obtained for the continuous-dimer case, as well as the dimer-perfect case. We can say that the system shows a

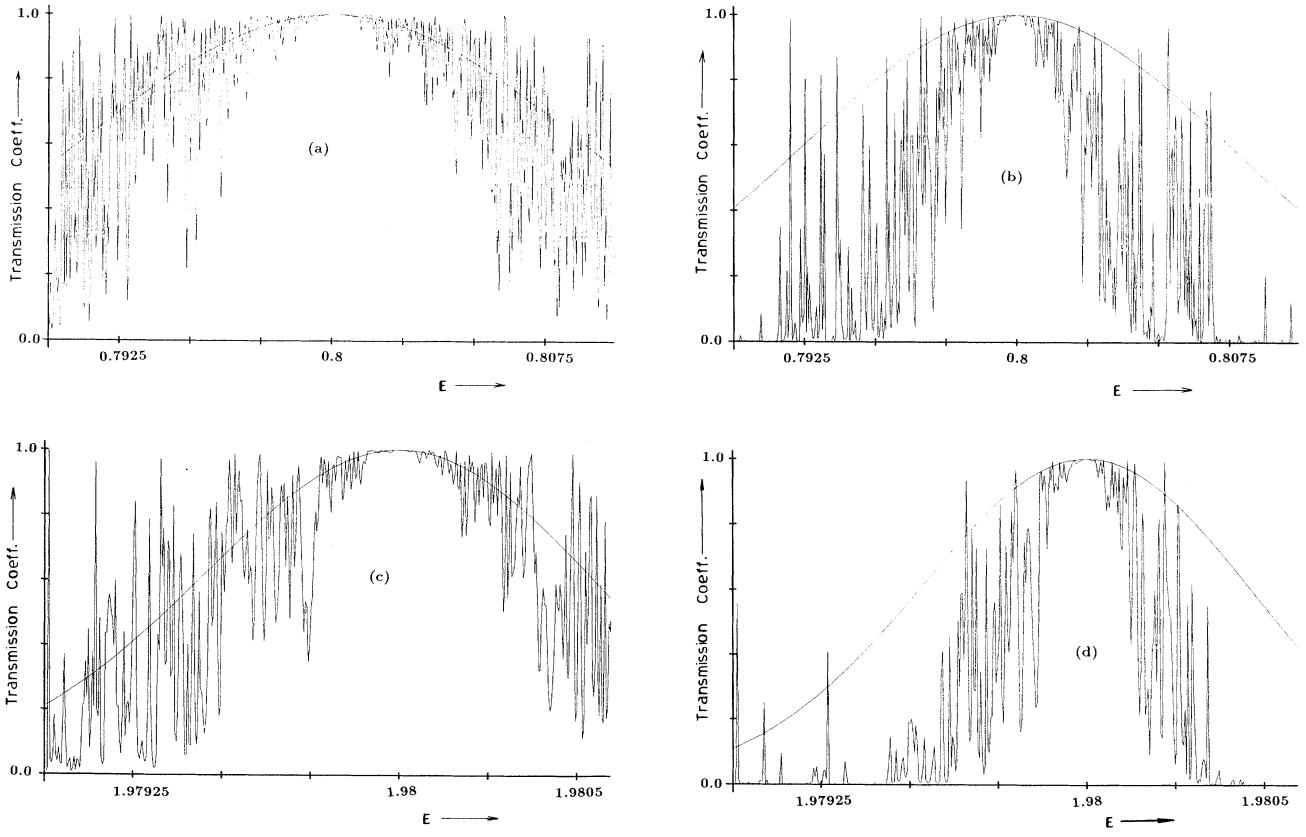

FIG. 6. (a) Transmission coefficient $|T|^2$ as a function of particle energy (E) for RDM with 10^5 lattice sites. The smooth curve corresponds to $|t|^{2p}$. The dimer energy is $\epsilon_0=0.8$ and the concentration is $\rho=0.33$. (b) Same as in (a) but $\epsilon_0=0.8$ and $\rho=0.47$. (c) Same as in (a) but $\epsilon_0=1.98$ and $\rho=0.33$. (d) Same as in (a) but $\epsilon_0=1.98$ and $\rho=0.47$.

tendency of forming a band around the dimer energy. This feature can be understood properly by studying the length dependence of the transmission coefficient around the dimer energy. When we consider the case of a particle energy (E) sufficiently away from the dimer energy, the transmission coefficient after a certain length, depending on the energy, rapidly decreases. As we proceed towards the dimer energy, the oscillatory behavior [shown in Figs. 8(a)–8(b)] of the transmission coefficient as a function of the sample size becomes more pronounced. This behavior of the transmission coefficient is an indication of the states having a localization length larger than the sample size. The region in this case lies within the energy range 0.795–0.805 and is roughly proportional to Γ_{eff}.

We next consider the case for large dimer concentration ($\rho=0.47$) and low energy ($\epsilon_0=0.8$). Here also the averaged transmission coefficient yields a Lorentzian curve. The half-width Γ_{fig} in this case is approximately Γ_{eff}. We also obtain a configuration-independent width (ΔE), where the transmission coefficient is approximately unity. This width is again an order of magnitude smaller than Γ_{eff}. We also consider the case when ϵ_0 is very close to one of the band edges ($\epsilon_0=1.98$). When the concentration is low ($\rho=0.33$), the averaged transmission coefficient again yields a Lorentzian curve with a half-width roughly equal to Γ_{eff}. On the other hand, for a high concentration, $\rho=0.47$, the half-width is substantially smaller than Γ_{eff}. Here again we find a configuration-independent width (ΔE). Note that the resonance width (Γ_{fig}) for the average transmission coefficient decreases with increasing dimer energy as well as dimer concentration. The configuration-independent width also decreases as Γ_{fig}. It is noticed that the number of resonance peaks significantly decreases around ΔE. We also examine the case when $\epsilon_0=1.9999$ and the concentration is $\rho=0.33$. Here we find that the configuration-independent width reduces significantly (see Fig. 9). It is actually proportional to $1/N$. In general, we find a discernable asymmetry in the configuration-independent width. It is noticed that the width is less in the side that is closer to the band edge.

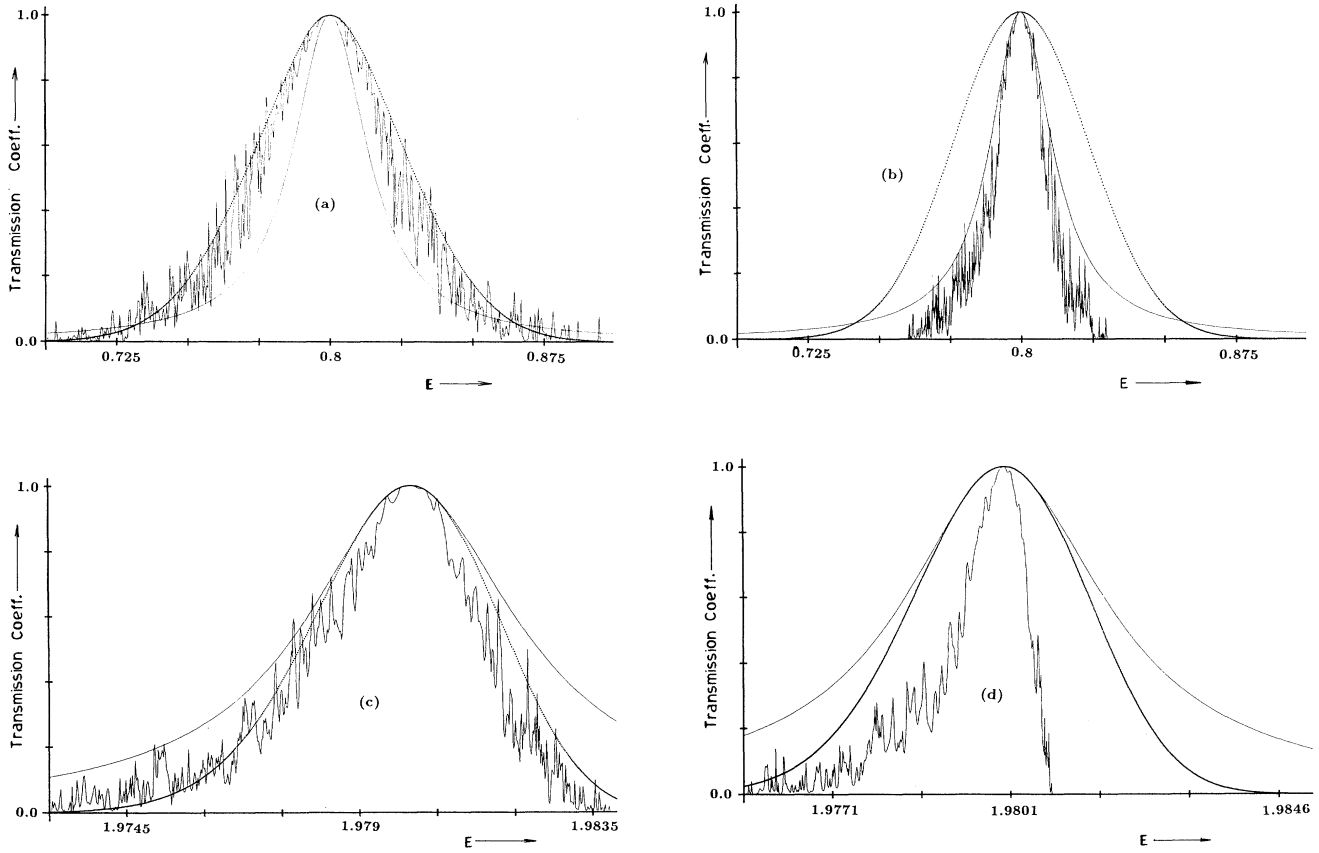

FIG. 7. (a) Arithmetic average of transmission coefficient ($\langle |T|^2 \rangle$) as a function of particle energy E for RDM with 10^4 lattice sites. The dotted curve corresponds to $\langle |t|^{2\rho} \rangle$ and the smooth solid curve is for

$$\left\langle \frac{1}{1+4(E-\epsilon_0)^2/\Gamma_{\text{eff}}^2} \right\rangle .$$

The dimer energy is $\epsilon_0=0.8$ and the concentration is $\rho=0.33$. (b) Same as (a) but $\epsilon_0=0.8$ and $\rho=0.47$. (c) Same as (a) but $\epsilon_0=1.98$ and $\rho=0.33$. (d) Same as (a) but $\epsilon_0=1.98$ and $\rho=0.47$.

Since localization due to disorder starts from the band edge, the side that is closer to the band edge will be affected more. This explains the observed asymmetry.

V. NUMBER OF NONSCATTERED STATES

The general remark in the study of the transmission coefficient is that the energy width ΔE and Γ_{fig} around ϵ_0 decreases with increasing dimer energy and concentration. We also find that for high concentrations and ϵ_0 well inside the band ($\rho=0.47$, $\epsilon_0=0.8$), and for low concentrations and ϵ_0 close to the band edge ($\rho=0.33$, $\epsilon_0=1.98$), the half-width obtained from our numerical calculations agree fairly well with Γ_{eff} which is $|2\sin k_0/\sqrt{\rho N}|$. Since $|T^2|\sim 1$ in the configuration-independent width (ΔE), we can assume that Bloch k is a good quantum number for these states. Also note that ΔE is roughly an order of magnitude smaller than Γ_{eff}. So, for these two cases we write

$$\Delta E = c_1 \Gamma_{\text{eff}} = c_1 \frac{\Gamma}{\sqrt{\rho N}} , \tag{21}$$

where c_1 is a constant. Since $E=2\cos k$ and the region of interest is infinitesimal, $\Delta E \sim 2\sin k_0 |\Delta k|$ and $|\Delta k| = 2\pi |\Delta N|/N$, where N is the number of sites in the sample. Now equating these two expressions for ΔE, we obtain $\Delta N \approx (c_1/2\pi\sqrt{\rho})\sqrt{N}$. This result agrees with DWP.[10] Note that the number of nonscattered states is of the order of $\sqrt{N}$.[16]

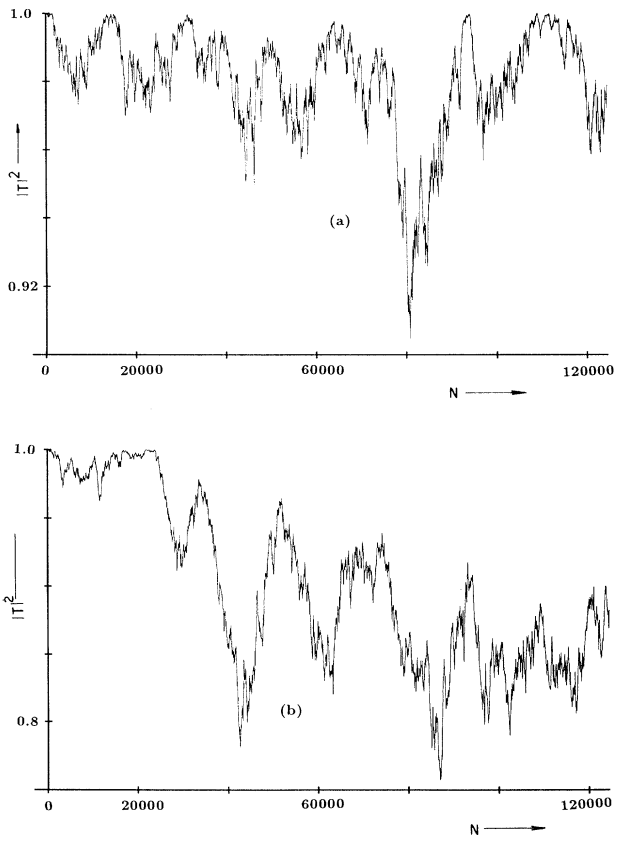

FIG. 8. (a) Transmission coefficient ($|T|^2$) as a function of sample size (N) for RDM with $E=0.795$, $\epsilon_0=0.8$, and $\rho=0.33$. (b) Same as (a) but $E=0.805$.

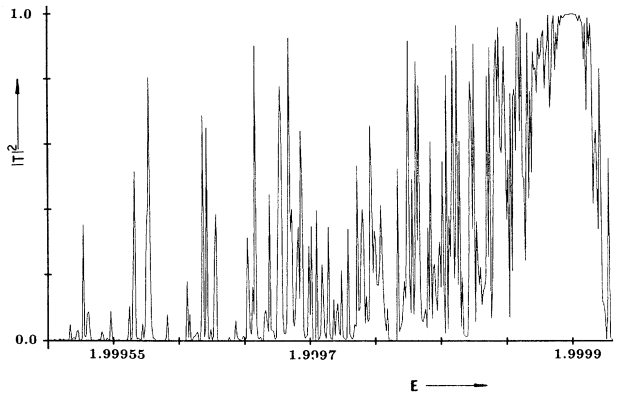

FIG. 9. $|T|^2$ as a function of E with dimer energy $\epsilon_0=1.9999$ and concentration $\rho=0.33$.

For all other cases (except at the band edge) we do find a discrepancy between the observed half-width (Γ_{fig}) and the calculated one (Γ_{eff}). If we ignore this discrepancy and equate ΔE with Γ_{eff} we obtain of the order of $\sqrt{N}$ ballistic-type states. We must also emphasize that the disagreement between these two half-widths should not be overlooked. This finding does not rule out the possibility that the observed half-width scales as $N^{-\lambda}$ where λ is function of both the concentration of dimers (ρ) and the energy of the dimer sites (ϵ_0). To check this possibility we investigated the case $\epsilon_0\sim 2$. Our analysis indicates that there will be only a finite number of extended states in the sample. Since this result lends credence to the hypothesis that the half-width scales $N^{-\lambda}$ with λ not necessarily $\frac{1}{2}$, further work in this matter is required.

We now explain the discrepancy between our results and that of Sen and Gangopadhyay.[33(a)] They found $N^{1/3}$ ballistic-type states while we believe that the number of such states will depend in general on the concentration and the energy of the dimer. This difference lies in the models studied. We investigated the DWP model.[10] In our model the random segment contains sites which also constitute the lead. In the other model[33(a)] the lead material is different from the materials inside the random segment. The essential behavior of the later model around any of the dimer energies can be understood from our continuous-dimer model. Note that in their case the scattering from the two leads is responsible for the sharpening of the resonance peaks around the dimer energies. On the other hand, in our model, scattering from the leads around the dimer energy is negligible. As a result, we do not see sharp resonances in the vicinity of the dimer energy. This shows that the nonscattered states around the dimer energy are very susceptible to extraneous scattering. Since the effect of the leads in their model will be negligible in an infinite system, we believe that in this limit two models will yield identical results.

VI. SUMMARY

To have an in depth understanding of RDM we first studied the phase and transmission coefficients of three simple models in the vicinity of the dimer energy (ϵ_0). These models predicted the merging of resonances in RDM around the dimer energy. This prediction was further substantiated by numerical analysis of phase and transmission coefficients of RDM for large samples. This observation can be understood by noting that at ϵ_0 our RDM reduces to a perfect crystal of infinite length. Hence, in the vicinity of ϵ_0, the appearance of nonscattered states must be observed. Of course, the width of these states must be determined by the extent of scattering. This, in turn, is determined by the energy and concentration of the dimer. In fact, we found that the averaged transmission coefficient yields a Lorentzian curve with a half width which depends on both the dimer energy and concentration of dimer in the sample. When the dimer energy is well inside the band and the concentration of dimers in the sample is high, the numerically observed value of the half width agrees nicely with theoretical prediction. The same kind of agreement is obtained when ϵ_0 is close to the band edge and the concentration is low. In these two situations we find that the number of nonscattered states is proportional to $\sqrt{N}$. Here, N is the number of sites in the sample. This result is in agreement with the result of DWP.[10] However, our numerical results indicate that the actual half-width, in general, may not be proportional to $1/\sqrt{N}$. Given the approximate nature of the derivation this discrepancy is not at all unlikely. Furthermore, when ϵ_0 is infinitesimally away from the band, we find that the average width is proportional to $1/N$. Since the disorder should start localizing states from the band edge, this finding is consistent with the physics of the problem. This also supports our conjecture regarding the number of nonscattered states. This aspect, however, will require further study.

It should also be noted that apart from a set of conducting states the system also contains a host of resonance states outside the configuration-independent width (ΔE). The number of such states increases significantly if either ϵ_0 or the concentration is decreased. This is definitely due to the reduction of scattering of the incoming waves by the sample. These resonance peaks will contribute to the mean-square displacement. They definitely play a prominent role in the mean-square displacement when ϵ_0 is very close to or at the band edge. Therefore, it is necessary to examine the behavior of the mean-square displacement for a low concentration of dimer with $\epsilon_0 \sim 2$ and the other extreme case when $\epsilon_0 \sim 0$ and the concentration is large. This work is in progress.

ACKNOWLEDGMENTS

We greatly appreciate many useful discussions with Dr. S. M. Bhattacharjee and Dr. A. K. Sen.

*Electronic address: kundu%iopb@shakti.ernet.in

[1] *Handbook of Conducting Polymers,* edited by T. A. Skotheim, (Dekker, New York, 1986).
[2] W. P. Su, J. R. Schrieffer, and A. J. Heeger, Phys. Rev. B **22**, 2099 (1980).
[3] J. Chen, A. J. Heeger, and F. Wudl, Solid State Commun. **58**, 251 (1986).
[4] F. Zuo, M. Angelopuolos, A. G. MacDiarmid, and A. J. Epstein, Phys. Rev. B **36**, 3475 (1987); **39**, 3570 (1989).
[5] L. W. Shacklette, J. F. Wolf, S. Gould, and R. H. Baughman, J. Chem. Phys. **88**, 3955 (1988).
[6] K. Mizoguchi, M. Nechtschein, J.-P. Travers, and C. Menardo, Phys. Rev. Lett. **63**, 66 (1989).
[7] D. S. Galvao, D. A. dos Santos, B. Laks, C. P. de Melo, and M. J. Caldas, Phys. Rev. Lett. **63**, 786 (1989); **65**, 527 (1990).
[8] H.-L. Wu and P. Phillips, Phys. Rev. Lett. **66**, 1366 (1991).
[9] P. Phillips and H.-L. Wu, Science **252**, 1805 (1991).
[10] D. Dunlap, H.-L. Wu, and P. Phillips, Phys. Rev. Lett. **65**, 88 (1990).
[11] P. Phillips, H.-L. Wu, and D. Dunlap, Mod. Phys. Lett. B **4**, 1249 (1990).
[12] P. W. Anderson, Phys. Rev. **109**, 1492 (1958).
[13] N. F. Mott and W. D. Twose, Adv. Phys. **10**, 107 (1961).
[14] R. E. Borland, Proc. Phys. Soc. **77**, 705 (1961); **83**, 1027 (1964).
[15] B. I. Halperin, Adv. Chem. Phys. **13**, 123 (1967).
[16] H. Matsuda and K. Ishii, Prog. Theor. Phys. Suppl. **45**, 56 (1970).
[17] R. Abou-Chacra, P. W. Anderson, and D. J. Thouless, J. Phys. C **6**, 1734 (1973).
[18] E. Abrahams, P. W. Anderson, D. C. Licciardello, and T. V. Ramakrishnan, Phys. Rev. Lett. **42**, 673 (1979).
[19] P. Erdös and R. C. Herndon, Adv. Phys. **31**, 65 (1982).
[20] M. Y. Azbel and P. Soven, Phys. Rev. B **27**, 831 (1983).
[21] C. Basu, A. Mookerjee, A. K. Sen, and P. K. Thakur, J. Phys. Condens. Matter **3**, 9055 (1991).
[22] B. Y. Tong, Phys. Rev. A **1**, 52 (1970).
[23] E. N. Economou and P. D. Antoniou, Solid State Commun. **21**, 285 (1977).
[24] J. B. Pendry, J. Phys. C **20**, 733 (1987).
[25] M. Kohmoto, L. P. Kadanoff, and C. Tang, Phys. Rev. Lett. **50**, 1870 (1983).
[26] M. Kohmoto, B. Sutherland, and C. Tang, Phys. Rev. B **35**, 1020 (1987).
[27] H. Hiramoto and M. Kohmoto, Int. J. Mod. Phys. B **6**, 281 (1992).
[28] J. C. Flores, J. Phys. Condens. Matter **1**, 8471 (1989).
[29] D. Dunlap, K. Kundu, and P. Phillips, Phys. Rev. B **40**, 10 999 (1989); D. Dunlap and P. Phillips, J. Chem. Phys. **92**, 6093 (1990).
[30] H.-L. Wu and P. Phillips, J. Chem. Phys. **93**, 7369 (1990).
[31] H.-L. Wu, W. Goff, and P. Phillips, Phys. Rev. B **45**, 1623 (1992).
[32] A. Bovier, J. Phys. A **25**, 1021 (1992).
[33] (a) S. Gangopadhyay and A. K. Sen, J. Phys. Condens. Matter **4**, 9939 (1992); (b) A. K. Sen, S. Gangopadhyay, and A. Kar Gupta (unpublished).
[34] Y. Liu and K. A. Chao, Phys. Rev. B **34**, 5247 (1986).
[35] G. Bayam, *Lectures on Quantum Mechanics* (Benjamin/Cummings, Menlo Park, CA, 1969).
[36] J. A. Stovneng and E. H. Hauge, Phys. Rev. B **44**, 13 582 (1991).